ELSEVIER

Contents lists available at ScienceDirect

Reliability Engineering and System Safety

journal homepage: www.elsevier.com/locate/ress





A nexus approach to infrastructure resilience planning under uncertainty

Rachel L. Moglen^{a,*}, Julius Barth^b, Shagun Gupta^a, Eiji Kawai^c, Katherine Klise^d, Benjamin D. Leibowicz^a

- a Operations Research and Industrial Engineering, University of Texas at Austin, 204 E Dean Keeton St, Austin, TX 78712, USA
- ^b Information, Risk, and Operations Management, University of Texas at Austin, 2110 Speedway, Austin, TX 78705, USA
- ^c Energy and Earth Resources, University of Texas at Austin, 2305 Speedway Stop C1160, Austin, TX 78712, USA
- d Energy Water Systems Integration, Sandia National Laboratories, PO Box 5800, Mail Stop 0750, Albuquerque, NM 87185-1137, USA

ARTICLE INFO

Keywords: Infrastructure hardening Resilience Stochastic optimization Disaster planning Critical infrastructure systems Energy-water nexus

ABSTRACT

Natural disasters pose serious threats to Critical Infrastructure (CI) systems like power and drinking water, sometimes disrupting service for days, weeks, or months. Decision makers can mitigate this risk by hardening CI systems through actions like burying power lines and installing backup generation for water pumping. However, the inherent uncertainty in natural disasters coupled with the high costs of hardening activities make disaster planning a challenging task. We develop a disaster planning framework that recommends asset-specific hardening projects across interdependent power and water networks facing the uncertainty of natural disasters. We demonstrate the utility of our model by applying it to Guayama, Puerto Rico, focusing on the risk posed by hurricanes. Our results show that our proposed optimization approach identifies hardening decisions that maintain a high level of service post-disaster. The results also emphasize power system hardening due to the dependency of the water system on power for water treatment and a higher vulnerability of the power network to hurricane damage. Finally, choosing optimal hardening decisions by hedging with respect to all potential hurricane scenarios and their probabilities produces results that perform better on extreme events and are less variable compared to optimizing for only the average hurricane scenario.

1. Introduction

The complex interactions between different CI systems are something we all experience in our day-to-day lives. The drinking water that flows from our taps depends on the electricity sector to power the purification and distribution processes. Transportation networks require electricity to operate traffic signals. The electricity we consume when we turn on the light may have been generated from hydropower, steam heated in a coal or natural gas power plant, or a nuclear plant cooled by water.

The interconnections between CI systems become more apparent when disasters occur. After a disturbance, limited resource availability stresses interdependencies between systems. This can cause failures in one system to cascade into the systems that depend on it, resulting in disruptions throughout the dependent systems [1]. CI systems are systems whose failure "would have a debilitating impact on the defense and economic security" of a nation [2]. This includes drinking and waste water, natural gas, telecommunications, transportation, electric power systems, and emergency services [1]. Recent worldwide disasters such as the 2001 World Trade Center attack, the 2011 Japan Earthquakes, the 2017 Puerto Rico hurricanes, and the 2021 Texas freeze

reveal both the interconnections between CIs and the importance of CIs to the functioning of our society [1,3,4]. In these and similar events, CI interdependencies include outages of traffic signals due to loss of electricity, loss of water pressure due to electricity loss at pumping stations, water main breaks from co-located utility failures, and disruption in communication services for emergency response and repair due to electricity and telecommunication system outages. Power outages result in \$20 to \$50 billion in damages annually to the United States (U.S.) economy alone, and data suggest that outages are becoming more frequent and more severe with time [5]. The frequency and impacts of natural disasters have exhibited nearly exponential growth in recent decades [6]. The growth of the world's population combined with the threat of climate change places more stress on already vulnerable infrastructure systems [6,7]. Therefore, disaster modeling and analysis of our CI and its vulnerabilities is an important and active area of study [1].

In this paper, we develop a decision-making framework that systems planners can use to make interconnected CI more resilient to a disaster or disturbance. Resilience is the ability of a system to withstand,

E-mail address: rmoglen@utexas.edu (R.L. Moglen).

^{*} Corresponding author.

absorb, adapt, and rapidly recover from disturbances like hurricanes. floods, earthquakes, and malicious attacks [1,6,8,9]. In this study, we focus on long-term resilience planning or mitigation, exploring the paradigm where decision makers seek to harden existing infrastructure. These hardening activities include repairing water pipe leaks, installing backup generation at pumping stations, undergrounding power lines, and protecting water storage facilities. The inherent uncertainty in predicting the occurrence and impact of natural disasters presents a key challenge in resilience planning [8]. In this work, we consider the impacts of natural disasters, specifically hurricanes, on connected power and drinking water infrastructure by modeling the problem as a two-stage stochastic program, a paradigm widely employed in the literature for disaster planning [10–12]. The first stage (here-and-now) decisions are the decision maker's investment decisions to make the systems more resilient to disturbances. The second stage (recourse) decisions are the operations that meet as much demand as possible, given a realization of the disturbance. In this study, we characterize the uncertainty in disaster realization through the capacities of infrastructure components after the disaster, which depend on the disaster scenario and the first stage hardening decisions. In contrast to other models employing scenario- or simulation-based approaches [13-18], we are thus able to develop an optimal decision-making framework that hedges with respect to potential disaster realizations and their probabilities. A cost-minimization objective forces decision makers to prioritize which components they choose to harden in the face of disaster uncertainty. The primary factors causing the model to identify an infrastructure component for hardening are trade-offs among its probability of failure, its criticality in being able to serve demand across infrastructure systems, and the relative cost of hardening the asset compared to the possible cost of repairing it.

In summary, our work contributes to the literature by:

- Developing a framework for identifying optimal hardening decisions across interdependent power and water infrastructure systems
- 2. Exploring the relationship between power and water infrastructure in a disaster context
- 3. Characterizing the uncertainty in natural disaster realization and the threats that disasters pose to power and water infrastructure
- Applying our framework to a detailed, empirically grounded case study to demonstrate its efficacy for real-world disaster planning

We implement our model for a case study based on the city of Guayama, Puerto Rico. In this case study, we demonstrate the ways our methods can be used to guide a decision maker's planning decisions by prescribing hardening actions they should undertake. At optimality, our model recommends more hardening of the power network than the water network. This phenomenon is driven both by the power network's greater vulnerability to hurricanes and the water network's dependency on power to treat its water supply. We find that hedging over potential hurricane scenarios yields decisions that are less variable and perform better in the event of extreme disasters relative to planning only for the average hurricane scenario, validating our advanced treatment of disaster uncertainty. We also find that system performance is largely insensitive to the relative cost of repairing assets versus hardening them. Finally, we find that service level requirements imposed by decision makers are able to be maintained across a wide variety of simulated disaster scenarios when optimal hardening is implemented.

The remainder of this paper is organized as follows. We provide an overview of the most relevant literature on resilience planning in Section 2, paying special attention to resilience planning for interdependent infrastructure systems. In Section 3, we present our two-stage stochastic programming formulation for the interconnected water-power resilience planning problem. We describe a case study of interdependent power and water infrastructure in Section 4, focusing on the city of Guayama, Puerto Rico. We then explore the case study results in detail in Section 5. Finally, we discuss our conclusions in Section 6.

2. Literature review

While this paper focuses specifically on the resilience of interdependent infrastructures, the resilience of individual infrastructure systems has a long history as an active area of interest in the literature. Works that focus on individual CI systems often model relationships that may be too computationally intensive in papers studying interdependent infrastructure systems. Power [3,10,19], drinking water [14,15], and transportation [11,12,16] infrastructure systems are most frequently studied in the literature. For example, power grid resilience work often captures nonlinearities of power flow using the AC or DC approximation, thus capturing the real-world response of these systems to disturbances [10,19]. The resilience literature adopts different planning horizons. Some work explores long-term hardening decisions that decision makers face months or years in advance to prepare for disasters [3], while other work focuses on short-term planning as system operators prepare for an upcoming disaster and then repair any damage made to the infrastructure, restoring service [12,16]. In the context of individual CI planning, researchers often take the perspective of the system operator or utility in their study [3,11,12]. In contrast, researchers in the interdependent infrastructure literature often take the perspective of a system-of-systems planner, such as the Federal Emergency Management Agency (FEMA), where the decision maker is coordinating responses across multiple systems [20]. In the case of the individual system planner, the objective may be more cost-based [11, 19], rather than the service-based objectives of system-of-systems planners. However, because individual CI utilities still serve the public good, they still typically evaluate the risk of lost service, either as part of the objective function or through a constraint [16,19]. While resilience planning for individual infrastructure systems can improve the computational tractability of models, the interactions between CI systems and their impacts on overall system performance [1] serve to motivate our nexus approach to CI planning.

Modeling of interdependent CI is a growing area of the literature. Some work has been done on interdependent CI modeling in a non-disaster context [21,22]. Because the interactions between interdependent CI become more apparent and relevant to system performance in the case of disasters, interdependent CI is typically studied in the context of resilience and emergency response. Classification and modeling of infrastructure interdependencies are discussed in [23]. [23] classifies interdependencies along two orthogonal dimensions: ontology and epistemology. The dimension of ontology describes when and how the interdependencies appear, whereas the dimension of epistemology classifies the interdependencies into modeling stages. [23] describes two classifications in the dimension of ontology: episodic (interdependencies that appear only under certain conditions) and chronic (interdependencies that always exist). We focus on a chronic interdependency; we assume that the water system depends on the power system to operate across our decision making time horizon. In the dimension of epistemology, [23] identifies four stages of the resilience modeling process: hazard and exposure, policy and control, operation and performance, and deterioration and recovery. Our framework spans the first three stages. First, we develop a hazard and exposure model to simulate the impacts of a hurricane on a network. Then, our model's first stage forms a policy and control model capturing the economic considerations of resilience planning. Finally, our model describes the operation and performance of the system for each disaster realization in the second stage.

There are five main approaches to modeling the resilience of interdependent CI systems in the literature: empirical approaches, agent-based approaches, system dynamics-based approaches, approaches based on economic theory, and network-based approaches. Ouyang [1] provides an in-depth comparison of the different approaches and their relative advantages and disadvantages. Empirical studies explore events from historic case studies after a disaster using both quantitative and qualitative approaches. In such studies, data are gathered from

a number of sources including newspapers and media reports [24], expert opinions [25], and utility owners and operators [26]. In these empirical studies, failure consequences are characterized both by their impact, defined by duration and severity, and their extent, defined by the geographic area and the population impacted [27]. Empirical studies range from system-level to component-level analyses [1]. By contrast, agent-based approaches use a bottom-up approach, modeling the complex behaviors of individual CI as individual agents interacting with other CI and their environment based on a set of rules [1]. This modeling paradigm is popular at the U.S. National Labs, with agent-based resilience modeling tools developed at Sandia National Labs [28], Argonne National Lab [29], and Idaho National Lab [30]. While agent-based modeling is a bottom-up paradigm, system dynamics approaches use a top-down modeling approach to capture the feedbacks between different CI [1]. The challenge presented by model structure selection, parametrisation, and model validation are all weaknesses of this modeling approach [1]. The fourth modeling approach to interdependent CI modeling is based on economic theory, e.g., Leontief models and equilibrium-based models. Under the Leontief input-output economic model [31] the impacts of a disturbance are captured as decreased output or level of service from one sector, and the model structure captures the impact of that sector on others. However, these models do not capture component-level interdependencies, and the matrix of sector interdependencies can be difficult to parameterize [1]. Economic theory-based approaches can also include equilibrium-based models capturing the behavioral responses of consumers and producers for infrastructure, e.g. [20]. Finally, network-based resilience models illustrate CI components as nodes and connections between nodes as links [1]. In these network-based studies, a hazard eliminates or reduces the capacities of nodes and edges, simulating the impacts of a disaster [9,17,32]. Some network-based approaches may explore network topology, such as connectivity changes and redundancies [33], while others model network flows, either as generic commodities [34] or including nonlinearities such as power and water flows [10,19,21]. As Ouyang [1] notes, network flow-based approaches capture operational mechanisms, providing more realism in system behavior than the other four modeling approaches. Our paper employs a network flowbased approach to resilience planning, modeling the flows in power and water infrastructure as generic commodities, a simplification that allows for more computationally-intensive modeling of other dimensions of the problem, such as uncertainty. We find that our rigorous treatment of uncertainty through two-stage stochastic programming produces hardening recommendations that perform better on extreme events and are less variable compared to optimizing for only the average hurricane scenario. This performance improvement helps justify our selection of a network-based approach and related modeling assumptions.

2.1. Treatment of uncertainty

In resilience planning, the treatment of uncertainty presents a significant modeling challenge due to the low probabilities, but high consequences, of many disaster types [1]. While some resilience work does not consider the uncertainty from natural disasters [20,35], most models include some notion of uncertainty in the analysis and decisionmaking framework. Treatment of uncertainty ranges from less rigorous, in the form of scenario-based analysis [17,18], to more rigorous simulation-based modeling [13-16], to the most rigorous approaches that include uncertainty hedging in the model structure, either through robust optimization [9] or two-stage stochastic programming [9-11, 36]. While scenario analysis and simulation are common approaches to disaster uncertainty modeling in the literature, they do not guarantee optimality of the actions they recommend, or even make clear the degree of suboptimality [10]. Therefore, in this study we employ twostage stochastic programming to fully embed uncertainty within the optimization framework. This paradigm guarantees that the solution it finds is optimal with respect to the set of disaster scenarios incorporated

into the stochastic program [37]. Frequently, there are many or infinite possible realizations of uncertainty, for example when the distribution of possible uncertainty realizations is continuous. In this case, it is common to use Monte Carlo methods to sample scenarios from the distribution of possible uncertainty realizations [37], called Sample Average Approximation (SAA). SAA does not guarantee optimality across all possible uncertainty realizations, though it does guarantee optimality across the specific scenarios that are sampled. It is for this reason that we employ an out-of-sample evaluation of the hardening decisions. We find that constraints imposed in the in-sample formulation are, with few exceptions, able to be met in the out-of-sample evaluation. This suggests that the SAA, and the number of scenarios we select in our approximation, are sufficient to fully characterize the uncertainty in disaster realization and deliver optimal or near-optimal hardening decisions.

For most paradigms, scenario generation is a key component of modeling uncertainty. Some papers employ an in-depth scenario generation process, relying on historical data to derive representative disaster scenario distributions [13,15,38]. Then a disaster scenario is sampled from the distribution, and fragility curves are used to ascribe the corresponding level of infrastructure damage to the sampled disaster magnitude [15,38]. Other works employ a more abstract process to define scenarios by directly sampling the amount of damage experienced by the infrastructure, generally from uniform, normal, or lognormal distributions [3,16]. We selected the former method for its higher degree of realism; an empirically-grounded case study is one of the contributions of this work. First, we sample a category of hurricane based on historical observations from our area of interest. Then we apply fragility curves to determine asset failure probabilities throughout the network. Last, we sample network damage realizations according to these computed failure probabilities.

While we largely focus on optimal decision making uncertainty, indeed this is the reason for our selected modeling paradigm, through sensitivity analysis we also consider the impact of uncertainty in our model parametrisation. This backwards propagation of uncertainty helps quantify the amount of uncertainty each uncertain aspect of the model and its inputs contribute to the overall uncertainty in the model's response [39]. [40] classifies sources of error in the resilience modeling process into sample error, uncertain inputs, and model error. We focus on input uncertainty by perturbing three model parameters: the system performance requirement, the relative cost parameter, and infrastructure prioritization. Often, the computational challenges of stochastic programming prohibit sensitivity analyses [11,41], while others include at least a sensitivity analysis of the impact of available budget [42,43] similar to the analysis we conduct on the impact of our three most uncertain model parameters. More rigorous sensitivity analysis techniques include Global Sensitivity Analysis (GSA) [39,40] and Reliability-Oriented Sensitivity Analysis (ROSA) [44]. These sensitivity analysis techniques can help guide future data collection by identifying characteristics of the system and hazards that contribute significantly to uncertainty [40] but were out of scope for this study.

2.2. Decision objectives

In this paper, as with all research in the resilience space, the objective has implications for system performance, cost, and fairness. Because many papers take the perspective of a system planner, maximizing system performance or minimizing service loss are the most common objectives [10,13,14,16,35]. Some works combine both cost-based and service-based objectives in their optimization problem by quantifying the financial cost or value of lost service [9,17,18]. In these works, the financial cost of hardening and disaster response is usually included in the objective, creating a cost-effectiveness framework. In our work, we choose to minimize total expected costs. We measure resilience using an unmet demand constraint bounded by a service level requirement, favoring a cost-effectiveness structure. We define

unmet demand as the difference between exogenous demand and the amount of a commodity (power or water) that is actually delivered. We selected this framework because it most closely matches the system planner's perspective. Fairness is typically considered in concert with other decision objectives, for example Karakoc et al. [17] normalize individual lost service by the social vulnerability of the individuals. Additionally, many works include a spatial dimension of their proposed resilience metrics quantifying the criticality of a node [9,14,32,45,46]. Node weighting can capture critical loads like hospitals, schools, and nursing homes, vulnerable populations, or differences in the importance of different infrastructure types. We include equity consideration and spatial resolution in our resilience metric through individualized node weighting, with a parameter describing the criticality of satisfying demand at each node in each infrastructure system. In our case study, we use this parameter to establish a prioritization between power and water unmet demand. Finally, a measure of risk is often included in resilience models, either as an expected value of service level [10-12], a worst-case service level [9], or another metric for recovery, such as the difference in minimum and maximum recovery times across simulations [16]. In our formulation, we impose the minimum service level requirement across all scenarios, thereby dictating that the worst-case unmet demand does not exceed the service level requirement.

2.3. Temporal resolution and planning horizon

The temporal dimension of resilience planning is another differentiating model characteristic in the literature. Resilience planning takes the form of long-term mitigation and short-term preparedness and repair. Mitigation, or long-term resilience planning, is where decision makers proactively improve the resilience of CI systems by either hardening existing components or by expanding networks to introduce redundancies [10,20]. Preparedness, the first step of short-term resilience planning, describes the process of staging disaster repair and response infrastructure such as gathering repair materials, installing temporary protection equipment like flood barriers, and operating CI to best prepare, for example by filling water storage tanks in advance of anticipated loss of service [12]. Repair or restoration, the second stage of short-term resilience planning, involves systematically restoring service by repairing damaged infrastructure [16-18]. Adaptation, a key component of resilience planning, means that service may not be restored to pre-disaster status [6]. Some works include a combination of long-term and short-term resilience planning [9,11]. In our work, we focus on long-term disaster planning or mitigation, but include the ability of the system operators to operate the systems differently in each realization of the disaster. This methodology is consistent with other two-stage stochastic programs implemented in the literature [10-12]. While we choose to model the resilience problem with two stages, one of which represents the post-disaster stage, other works in the literature explore multiple time periods [9,13,15-19,32,35,45-49]. These works generally model the restoration and repair logistics of CI, therefore necessitating the multi-stage approach. The computational complexity this entails generally requires simulation or other non-prescriptive methods, which does not guarantee optimal decision-making guidance. In contrast, our model does guarantee optimality of hardening decisions with respect to the set of disaster scenarios included in the stochastic program, as previously discussed. Restoration-focused works like [47, 48] may feature more computationally-intensive modeling assumptions like binary decision variables and restoration crew scheduling. Conversely, we assume all decision variables are continuous, making our model a Linear Program (LP) as compared to the Mixed Integer Linear Program (MILP) explored in [47,48]. This difference is in part because detailed modeling of crew scheduling requires the use of binary variables to define assignments, while hardening decisions are closer to continuous. Decision makers face a range of hardening options in terms of cost (e.g., tree trimming versus burying power lines) and spatial resolution (i.e., hardening only a portion of a link). Additionally, restoration

models typically prescribe rebuilding sequences for a specific disaster realization. In comparison, the hardening problem explored in this paper identifies a resilience plan that is optimal with respect to the set of all disaster scenarios, though represents a significant additional computational burden. Thus, by assuming that hardening decisions are continuous, we not only capture some of the range in possible hardening decisions, but are also able to prescribe decisions that are optimal across a range of disaster scenarios.

2.4. Case study selection

We demonstrate our proposed framework on a detailed real-world case study, a primary contribution of this work. We represent the city of Guayama, Puerto Rico with a combined 2203 nodes and 2468 edges for the power and water systems, making our case study among the largest that we have found in the literature [11]. With this scale, we are able to demonstrate our model's efficacy for real-world disaster planning. Many other case studies demonstrate their models on networks with around 100 or fewer nodes [9,17,19,32], often on synthetic examples [18,21,35,50]. Our ability to implement our model on a realworld case study was aided by the availability of public data from the government of Puerto Rico [51]. As noted by Ouvang [1], data access is a fundamental problem in CI modeling, in part driving the selection of our case study. A symbiosis can exist between stakeholders and researchers that we hope to see leveraged as the field of CI resilience modeling grows. In our case study, we also develop scenarios tailored to real-world disasters, specifically hurricanes. The disaster types explored in the literature include hurricanes [13,19], earthquakes [11,12,14-17,32], and generalized infrastructure disturbances [3,9,18,20]. The disaster type selected is usually motivated by the geographic region of the case study. In our case, hurricanes pose a severe threat to Puerto Rico, a fact highlighted by the 2017 Category 5 hurricanes Irma and Maria [3]. Our disaster scenario generation algorithm is therefore designed to simulate the effects of hurricanes on the network in Guayama, Puerto Rico.

3. Formulation

We construct the resilience hardening problem as a two-stage stochastic program. This modeling paradigm is well-suited for modeling disaster planning problems, capturing both the planning decisions made before the realization of the uncertain natural disaster and the operational decisions made in the aftermath. We assume that there is a central decision maker allocating funds to the water network and power network and that there is coordination between power and water hardening decisions. Fig. 1 illustrates the conceptual relationship between the power and water networks ideated in this study. Power generation (Red "G") and reservoir (Blue "R") nodes represent the supply nodes in the power and water networks, respectively. The red "R" node in the power network corresponds to the power demand for water treatment. Ovals are demand nodes, denoting either individual customers or aggregations at the neighborhood scale. Demand nodes may or may not have non-zero demands, shown by the presence of a "D". Thick dashed lines in the water network in Fig. 1 represent pumps, and the linkage between these assets and pump stations ("P") in the power network. If a disaster occurs, then the capacities of certain system assets - power stations, water reservoirs, water pumps, water links, and power links - can be reduced if these assets are not sufficiently hardened. Our framework allows the system planner to hedge their hardening decisions with respect to a probability distribution of potential disaster realizations. We model the system planner's primary objective as minimizing expected costs, consisting of preparedness and expected repair expenditures, given a required service level. The flexibility of our proposed framework allows the system planner to assign weights to service losses, thereby prioritizing specific loads and infrastructure types.

Тa	bI	e	1			
				1		

Nomenclature.	
Sets and Indices	
$s \in S$	Infrastructure systems $S = \{W \cup P\}$ where W is water and P is power
$i \in \mathcal{N}^s$	Nodes $\mathcal{N}^s = \{\mathcal{N}^W \cup \mathcal{N}^P\}$ in infrastructure system network $s \in S$
$(i,j) \in \mathcal{E}^s$	Edges $\mathcal{E}^s = \{\mathcal{E}^W \cup \mathcal{E}^P\}$ in infrastructure system network $s \in S$
$\omega \in \Omega$	Disaster scenarios characterized as realized network failures
Decision variables	
y_i^s z_{ij}^s $u_{i\omega}^s$	First stage node hardening decisions for node i
z_{ij}^s	First stage edge hardening decisions for link (i, j)
$u_{i\omega}^s$	Second stage nodal unmet demand at node i under scenario ω
$x_{ij\omega}^s$ $\sigma_{i\omega}^s$ $\tau_{ij\omega}^s$	Second stage link flowrates for link (i, j) under scenario ω
$\sigma^s_{i\omega}$	Second stage node supply capacity used under scenario ω for node i
$\tau^s_{ii\omega}$	Second stage fraction of link capacity available (undamaged) under scenario ω for link (i,j)
$\theta_{i\omega}^{s}$	Second stage fraction of node capacity available (undamaged) under scenario ω for node i
$\rho_{i\omega}$	Second stage endogenously calculated power demand at node i required by the water
	system in scenario ω
Parameters	
d_i^s	Demand on infrastructure system $s \in S$ at node i
p_{ω}	Occurrence probability of disaster scenario ω
w_i^s	Weight placed on node i's unmet demand for system s
c_i^s , c_{ij}^s	Hardening cost for nodes i and links (i, j) , respectively, in system s
\bar{c}_i^s , \bar{c}_{ij}^s	Repair cost for nodes i and links (i, j) , respectively, in system s
U	Allowable weighted service level of the two systems across scenarios ω
κ_i^W, Q_{ij}^W	Power-dependent supply capacity at node i and link (i, j) , respectively
a_{ik}	Conversion of power to water flowrate for water treatment. 0 if $[i, k]$ is not a mapping
	between water treatment plant i and k in the water and power networks, respectively
b_{ijk}	Conversion of power to water flowrate for pumping. 0 if $[(i, j), k]$ is not a mapping between
•	pump stations (i, j) and k in the water and power networks, respectively
$\psi^s_{i\omega}, \xi^s_{ij\omega}$	Realization of undamaged fraction without hardening under scenario ω for nodes i and
-	links (i, j) , respectively. 0 if asset has failed, 1 otherwise

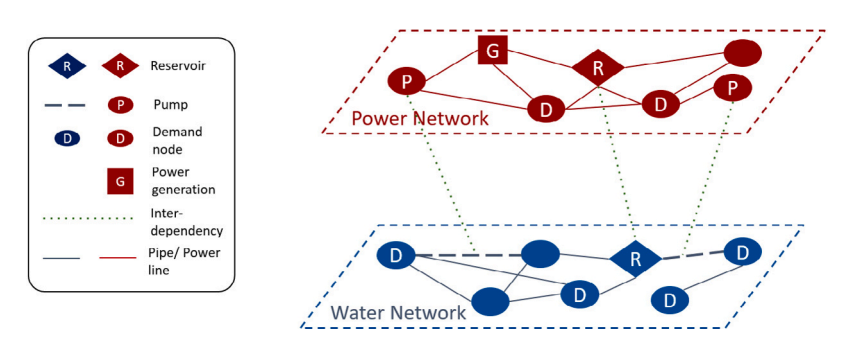


Fig. 1. Conceptual model of power-water network interdependencies.

The system planner's decisions consist of first stage "here-and-now" planning decisions and second stage "recourse" decisions. We model the problem using interconnected infrastructure systems $s \in S =$ $\{W \cup P\}$ where W is the drinking water infrastructure and P is power infrastructure. These systems are fundamentally networks consisting of nodes $i \in \mathcal{N}^s$ and links $(i, j) \in \mathcal{E}^s$ going from node $i \in \mathcal{N}^s$ to node $j \in \mathcal{N}^s$ for system $s \in S$. Continuous first stage variables y_i^s capture the amount of hardening done at each node i. Additional continuous first stage variables z_{ii}^s represent the amount of hardening done on the link (i, j). Both y_i^s and z_{ij}^s are bounded between 0 and 1, describing the fraction of original capacity that is protected by hardening. The bounds on the hardening decision variables could be tightened by decision makers to better match their fragility assessments. Fractional hardening can be interpreted as investment in either less expensive hardening activities or only partial hardening along a link. Nonlinear representations of the impact of mitigation exist in the literature [42,43], though these studies are computationally limited to smaller case studies or heuristic methods. The planner's second stage decisions focus on operation of the networks after the realization of the disaster scenario $\omega \in \Omega$. We model this as a multi-commodity network flow problem, with $x_{ii\omega}^s$ representing the flow along link (i, j) in infrastructure system s under scenario ω . The variable $u_{i\omega}^s$ denotes the unmet demand under scenario ω at node *i* in system *s*. The fractions of node and link capacity available

(i.e., undamaged) under scenario ω , respectively, are represented by $\theta_{i\omega}^s$ and τ_{iio}^s . The amounts of nodal and link capacity used are represented by $\sigma_{i\omega}^{s,j\omega}$ and $x_{ij\omega}^{s}$, respectively. Finally, the second stage decision variable $\rho_{i\omega}$ captures the nexus power consumption at node $i \in \mathcal{N}^P$, which is the endogenously calculated power demand required by the water system. The nomenclature used in this paper is summarized in Table 1.

$$\min \sum_{s \in S} \sum_{i \in \mathcal{N}^s} c_i^s y_i^s + \sum_{s \in S} \sum_{(i,j) \in \mathcal{E}^s} c_{ij}^s z_{ij}^s + \sum_{\omega \in \Omega} p_{\omega} \left[\sum_{s \in S} \sum_{i \in \mathcal{N}^s} \bar{c}_i^s (1 - \theta_{i\omega}^s) + \sum_{s \in S} \sum_{(i,j) \in \mathcal{E}^s} \bar{c}_{ij}^s (1 - \tau_{ij\omega}^s) \right]$$

$$(1)$$

$$\sum_{s \in S} \sum_{i \in \mathcal{N}^s} w_i^s \frac{u_{i\omega}^s}{\sum_{j \in \mathcal{N}^s} d_j^s} \le U \qquad \forall \omega \in \Omega$$
 (2)

$$z_{ij}^{s} = z_{ji}^{s} \qquad \forall s \in S, (i, j) \in \mathcal{E}^{s}$$

$$z_{ij}^{w} + \sum_{j} z_{ij}^{w} - \sum_{j} z_{ij}^{w} + d_{ij}^{w} - u_{ij}^{w}$$

$$z_{ij}^{w} + \sum_{j} z_{ij}^{w} - \sum_{j} z_{ij}^{w} + d_{ij}^{w} - u_{ij}^{w}$$

$$z_{ij}^{w} + \sum_{j} z_{ij}^{w} - \sum_{j} z_{ij}^{w} + d_{ij}^{w} - u_{ij}^{w} -$$

$$\begin{split} z_{ij}^{s} &= z_{ji}^{s} & \forall s \in S, (i,j) \in \mathcal{E}^{s} \\ \sigma_{j\omega}^{W} &+ \sum_{i|(i,j) \in \mathcal{E}^{W}} x_{ij\omega}^{W} &= \sum_{i|(j,i) \in \mathcal{E}^{W}} x_{ji\omega}^{W} + d_{j}^{W} - u_{j\omega}^{W} & \forall j \in \mathcal{N}^{W}, \omega \in \Omega \end{split}$$

$$\sigma_{j\omega}^{P} + \sum_{i|(i,j)\in\mathcal{E}^{P}} x_{ij\omega}^{P} = \tag{4}$$

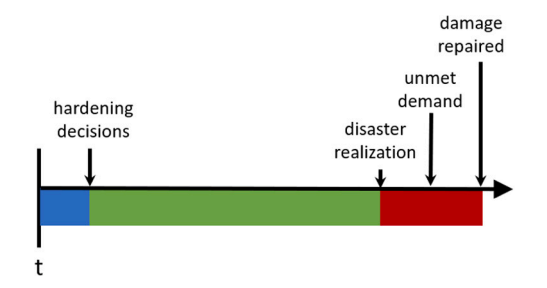


Fig. 2. Event sequence in the system planner's disaster hardening problem.

$$\sum_{i|(j,i)\in\mathcal{E}^P} x_{ji\omega}^P + d_j^P - u_{j\omega}^P + \rho_{j\omega} \qquad \forall j\in\mathcal{N}^P, \omega\in\Omega$$

(5)

$$a_{ik}\sigma_{i\omega}^{W} \le \rho_{k\omega} \qquad \forall i \in \mathcal{N}^{W}, k \in \mathcal{N}^{P}, \omega \in \Omega$$
 (6)

$$b_{ijk} x_{ij\omega}^{W} \le \rho_{k\omega} \qquad \forall (i,j) \in \mathcal{E}^{W}, k \in \mathcal{N}^{P}, \omega \in \Omega$$
 (7)

$$\theta_{i\omega}^{s} \le \psi_{i\omega}^{s} + y_{i}^{s} \qquad \forall s \in S, i \in \mathcal{N}^{s}, \omega \in \Omega$$
 (8)

$$\tau_{ij\omega}^{s} \le \xi_{ij\omega}^{s} + z_{ij}^{s} \quad \forall s \in S, (i,j) \in \mathcal{E}^{s}, \omega \in \Omega$$
 (9)

$$\tau^{s}_{ij\omega} = \tau^{s}_{ji\omega} \quad \forall s \in S, (i, j) \in \mathcal{E}^{s}, \omega \in \Omega$$
 (10)

$$0 \le y_i^s \le 1 \qquad \forall s \in S, i \in \mathcal{N}^s \tag{11}$$

$$0 \le z_{ij}^s \le 1 \qquad \forall s \in S, (i,j) \in \mathcal{E}^s \tag{12} \label{eq:12}$$

$$\rho_{i\omega} \ge 0 \qquad \forall i \in \mathcal{N}^P, \omega \in \Omega \tag{13}$$

$$0 \le x_{ij\omega}^s \le Q_{ij}^s \tau_{ij\omega}^s \qquad \forall s \in S, (i,j) \in \mathcal{E}^s \omega \in \Omega$$
 (14)

$$0 \le \sigma_{i\omega}^s \le \kappa_i^s \, \theta_{i\omega}^s \qquad \forall s \in S, i \in \mathcal{N}^s, \omega \in \Omega$$
 (15)

$$0 \le u_{im}^W \le d_i^W \qquad \forall i \in \mathcal{N}^W, \omega \in \Omega \tag{16}$$

$$0 \le u_{i\omega}^P \le d_i^P + \rho_{i,\omega} \qquad \forall i \in \mathcal{N}^P, \omega \in \Omega$$
 (17)

$$0 \le \theta_{i\omega}^{s} \le 1 \qquad \forall s \in S, i \in \mathcal{N}^{s}, \omega \in \Omega$$
 (18)

$$0 \le \tau_{ij\omega}^{s} \le 1 \qquad \forall s \in S, (i, j) \in \mathcal{E}^{s}, \omega \in \Omega$$
 (19)

We model all decisions using continuous decision variables, making our two-stage stochastic program an LP. The objective function (1) minimizes the total expected cost of first stage hardening and postdisaster repairs applied to the two CI systems. Constraints (2) place service level limits on the system across all scenarios ω , normalized by the total demand across the whole infrastructure network s. Critical nodes i for a specific infrastructure system s can be prioritized using the weighting parameter w_i^s as we demonstrate in our experiments. Decision makers can also adjust these weighting parameters w_i^s for vulnerable or otherwise disadvantaged populations to include equity consideration in their hardening plan. Constraints (3) impose symmetry of hardening in both link flow directions, because the decision variables correspond to a single section of pipe or power line that can be hardened, regardless of flow direction. Constraints (4) and (5) establish flow balance at all nodes in the water and power systems, respectively. Constraints (5) include the additional variable $\rho_{i\omega}$ capturing the endogenous power demand required by the water system. Constraints (6) bound the drinking water supply by the electricity available to treat it. Similarly, (7) constrain pump capacity by the amount of power available. Constraints (8) and (9) determine the realized capacities of nodes and links to supply demand and permit flow, respectively, based on the disaster realization and the first stage hardening decisions. Constraints (10) impose symmetry of link status. Constraints (11) through (19) impose bounds on the decision variables.

Depending on the parametrisation of the model, our formulation can model the system planner's problem across a variety of different disasters. Each disaster scenario is characterized by infrastructure failure realizations $(\psi^s_{io}, \xi^s_{iio})$ and occurrence probability p_ω . These scenarios

represent the next upcoming disaster for which the planner is preparing. Fig. 2 illustrates the sequence of events in the system planner's problem. The system starts in a pre-hardened state (blue in Fig. 2). Once the planner makes their hardening decisions, the system is hardened (green in Fig. 2). Then, a disaster occurs, resulting in unmet demand, and requiring repairs, inducing the damaged state (red in Fig. 2). The planner's constraint on system service level, i.e., unmet demand, is assessed before damage is repaired. While Fig. 2 shows a timeline, we assume steady-state network flow conditions in our assessment of unmet demand after the disaster realization. We also assume that after every disaster, the network is repaired to full working order. At its core, our formulation adopts a cost-effectiveness point of view where the system's desired service level is set at level U (constraints (2) will be binding for one or more scenarios). An alternative formulation would pose the problem as a cost-benefit study where constraints (2) enter the objective function and a value of lost service is used to assign a monetary cost to unmet demand.

Our model formulation employs simplifications to improve its computational complexity. We acknowledge these limitations but feel the trade-off is justified by the scale of the problem they allow us to explore. On the power side, common approaches to power system modeling include the AC or DC power flow problem. Phenomena like frequency control may also be included in these high fidelity operation models. On the water side, our model ignores energy constraints, water storage, and pipe friction losses. Some of these limitations may become more significant in a disaster context when the networks are stressed. For example, [52,53] develop high fidelity failure and operational modeling representations of interdependent infrastructure. However, with this level of detail, [52,53] are not able to rigorously explore the impacts of uncertainty on optimal resilience planning as we do in this paper. Furthermore, as noted in Section 2, simplifications like the ones we make in our model are not without precedent [1]. These simplifications are sufficient to capture operational mechanisms in a model whose focus is long-run planning, while avoiding the large computational burden of detailed mechanisms like energy balances [1]. Moreover, these simplifications allow us to more fully explore other dimensions of disaster modeling, such as the uncertainty of disaster impacts on a real-world sized network, while determining optimal here-and-now hardening decisions.

4. Case study

A significant and novel contribution of this work is the development of a large-scale case study involving a detailed representation of both power and water infrastructure, and therefore our framework's ability to aid real-world decision makers. As discussed in Section 2, many works either focus on an individual CI, do not employ optimization to provide prescriptive guidance to decision makers, or demonstrate their models only on small-scale synthetic examples. We address this gap by demonstrating our optimization framework's efficacy through a case study of the city of Guayama in Puerto Rico. Guayama, shown in Fig. 3, is a city located on the southeastern coast of Puerto Rico. The Guayama Municipality has a population of 45,362 as per the 2010 census [54]. Our AOI includes a portion of the Guayama Municipality extending from the more sparsely-populated northwestern reaches, south to the city center, and west along the coast. The AOI for our study contains a population of 20,394 [54]. As with all of Puerto Rico, Guayama is vulnerable to a number of natural disasters, including earthquakes, landslides, and hurricanes. In particular, hurricanes constitute a significant threat to the region, demonstrated by the 2017 Category 5 hurricanes Irma and Maria that left many without power or water for months. In this study, we focus on the threat hurricanes pose to Guayama, Puerto Rico.



Fig. 3. Case study AOI shown in green.

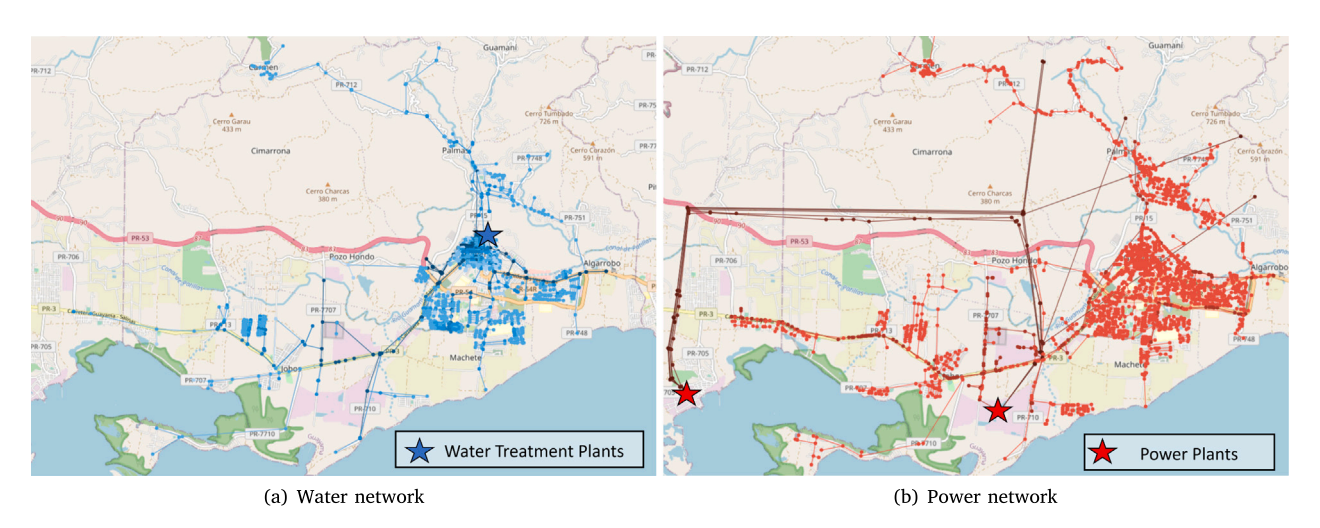


Fig. 4. Case study networks.

4.1. Guayama power and water networks

The network topology used in this case study comes from data made publicly available by the Government of Puerto Rico [51]. For our region of interest, the water utility is Puerto Rico Aqueducts and Sewers Authority (PRASA), and the power utility is Puerto Rico Electric Power Authority (PREPA). From our communications with PRASA, the two entities operate independently, but do work together to coordinate disaster preparedness and response.

Fig. 4(a) illustrates the water network used in our case study. Darker nodes and edges indicate larger diameter pipes. This network has one water treatment plant located in the northeastern part of the city: Guayama Urbano with a capacity of 6 million gallons/ day (0.26 m³/s). The water network is composed of approximately 200 km of pipes with 859 nodes and 1095 edges. 13 pumping stations are located throughout the network. Pipes range in diameter from 2 inches (5.08 cm) to 24 inches (60.96 cm). Nodal water demands were populated from 2010 census data [54] and an estimated per-capita residential water consumption of 51.46 gallons/ day (2.255 × 10^{-6} m³/s) [55]. Thus, the network's total population of 20,394 [54] generated 738.80 gallons/ minute (0.0466 m³/s) of drinking water demand.

Fig. 4(b) shows the power network used in our case study. This network has two power plants. The larger one, Complejo Aguirre, is located in the western region of Guayama and is connected to the power distribution system (light red) by transmission lines (darker red). Complejo Aguirre is an oil-fired plant with a capacity of 1540 MW. The second power plant, AES, is a coal-fired plant located in the southern part of Guayama and has a capacity of 454 MW. The power network

has 370 km of transmission and distribution power lines with 1344 nodes and 1373 edges. The power demand at each node was again parameterized based on the population of the surrounding area [54]. We calculated the demand on the network to be about 11.76 MW based on a population of 20,394 [54] and an average instantaneous residential power use of 576 W per-capita [56].

We employ synthetically generated hardening and repair costs in our case study, informed by the rough order of magnitude of costs found in the literature [57–59]. In reality, hardening and repair costs are highly variable, depending on the existing condition of infrastructure, the geographic region being studied, the specific hardening and repair methods selected, and the extent of damage [60]. Furthermore, because costs appear only in the objective function of our formulation, their absolute values do not impact the optimal solution, and only relative cost differences affect decision making. Therefore, one of our sensitivity analyses focuses on the repair cost factor R given in (20) and (21).

$$\bar{c}_i^s = Rc_i^s \tag{20}$$

$$\bar{c}_{ij}^s = Rc_{ij}^s \tag{21}$$

We assume that the hardening cost of power lines is \$10/m. This cost is of the same order of magnitude as activities like vegetation trimming and line inspection in [58]. We parameterize the hardening cost of power plants as \$1 million. This power plant hardening cost is based on the repair costs listed in [57]; we assume that power plant hardening costs can be of the same order of magnitude as repairs in our base case parametrisation. The hardening cost of water pipes is

assumed to be \$100/m [59] and water treatment plant hardening is assumed to be \$1 million. As previously mentioned, our formulation permits fractional hardening of both nodes and edges (y_i^s and z_{ij}^s are continuous decision variables) indicating investment in less hardening spatially or in less expensive activities. Because all costs in our model are variable costs, the costs listed above are the maximum cost of the activity (i.e., if the corresponding decision variable equals 1). Realworld hardening is more discrete than is modeled in this paper and includes fixed costs rather than exclusively variable costs. Therefore, costs for the actions prescribed by our model may be higher when they are actually implemented.

4.2. Hurricane scenario generation

In this study, we explore the threats that hurricanes pose to CI. Hurricanes constitute a significant threat to the region. Since 1851, Puerto Rico has been hit by six Category 4 or 5 hurricanes [61]. In the 170 years of data available in the National Oceanic and Atmospheric Administration (NOAA) database [61], 31 hurricanes have passed within 100 km of Guayama. Of those hurricanes, 11 were Category 1 as they passed our AOI, eight were Category 2, six were Category 3, three were Category 4, and three were Category 5. From these historical storms, we estimate that the next hurricane's severity will be Category 1 with probability 35.4% (11/31), Category 2 with a 25.8% (8/31) chance, Category 3 with probability 19.4% (6/31), or a Category 4 and 5 storm each with a probability of 9.7% (3/31). While we parameterize the distribution of hurricane severities based on historical occurrences, as in [38], the probability of extreme storms is increasing, driven by climate change. Decision makers looking to hedge against the changes could easily modify the distribution of hurricane severities to match a future climate change scenario.

We assign asset failure probabilities for both infrastructures based on the most common failure mode for the specific type of infrastructure in a hurricane. For electrical power systems, high winds, specifically wind gusts, cause the most damage to infrastructure. Water system infrastructure is most vulnerable to flooding [62], which in the coastal city of Guayama is largely caused by storm surge. In power infrastructure, winds bring down above-ground support structures for power lines and falling branches or trees can knock down the power lines themselves. Hurricane severity is defined on the Saffir-Simpson scale by the hurricane's sustained wind speed. Category 1 storms produce speeds 74-95 mph (119-153 km/h), Category 2 storms produce speeds 96-110 mph (154-177 km/h), Category 3 storms are "devastating" with speeds 111-129 mph (178-208 km/h), and Category 4 (speeds 130-156 mph (209-251 km/h)) and Category 5 (speeds greater than 157 mph (252 km/h)) are "catastrophic" [61]. For a given hurricane category, we assume that the wind gust speed (W_s) is approximately 25% higher than the sustained wind speed [60]. [38] defines the failure probability (Pr(failure)) of a transmission pole as (22) with 230 m between poles and the probability of distribution pole failure as (23) with an average 42 m between support poles. For both equations, W_s is assumed to be in mph. Eqs. (22) and (23) are visualized in Fig. 5.

$$Pr(transmission pole failure) = min\{(2E - 7)exp(0.0834W_s), 1\}$$
 (22)

$$Pr(distribution pole failure) = min\{0.0001 exp(0.0421W_s), 1\}$$
 (23)

These values were calibrated in [60] for Harris County, Texas which experiences a similar frequency of hurricanes as Puerto Rico and is also located in the United States. Therefore, we use the same parametrisation in our implementation. By dividing the length of each link in the power network by the distance between support poles, we obtain the number of support poles (N) for that link. We assume that the failure of each support pole is independent, and that the whole link will fail if any of the support poles along its length fail. We assume no spatial correlation between nearby power lines, instead generating the realization of each link failure as a Bernoulli random variable (RV)

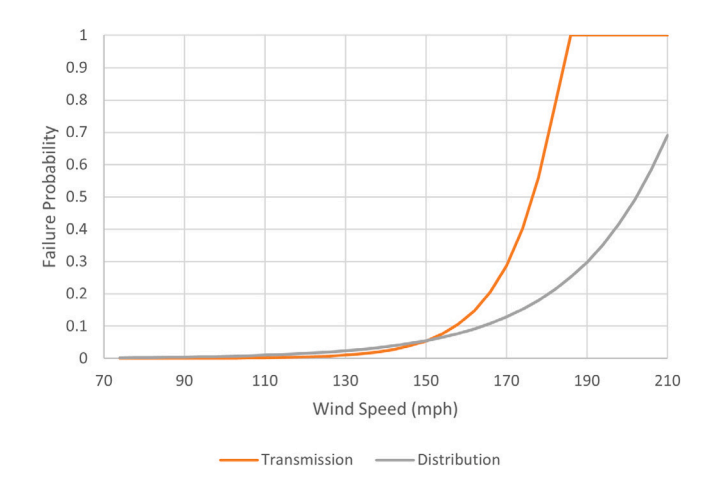


Fig. 5. Support pole failure probabilities.

with a failure probability calculated using (24). This procedure results in a 91.4% power line failure rate with a Category 5 hurricane in our case study. This value is similar to the 80% power system failure rate observed in the wake of Irma and Maria [3].

$$Pr(link failure) = 1 - (1 - Pr(support pole failure))^{N}$$
(24)

Water infrastructure is naturally more protected from hurricanes than power infrastructure, because it is typically below ground, protected from wind and falling trees. Its primary direct vulnerability is from flooding [62]. Indirect vulnerabilities due to CI interdependencies are also captured by our model, such as loss of power at pump stations for water treatment. As a coastal city, Guayama's primary flooding risk comes from storm surge. Fig. 6 shows the Category 1 and Category 5 storm surge zones, a NOAA data product generated using their Sea, Lake, and Overland Surges from Hurricanes (SLOSH) model [63]. By intersecting the water distribution network with these storm surge maps, we determine the inundation depths under Category 1 to Category 5 hurricane scenarios along all water pipes. As seen in Fig. 6(b), even in the most severe hurricane scenario, most of the infrastructure is outside the storm surge zone. Still, inundation depths up to 11 ft are possible in the AOI. We assume an inundation depth of 0.5 m or greater causes damage to the water infrastructure [62], and assume deterministic failure if flood depths exceed this threshold. No critical assets such as water treatment plants, pumps, or power stations fall in any storm surge zones in our case study's AOI.

Algorithm 1 details the scenario generation process. First, the user determines the number of scenarios desired. In our implementation, we generate $|\Omega| = 50$ scenarios to determine the system planner's optimal hardening decisions. Then, the storm severity for each scenario is generated. Next, for the power network, link failure probabilities are calculated using (22), (23), wind speeds for the scenario's storm severity, and the length of the link. Then, power link failure realizations are generated Bernoulli RVs. Pipe outages are determined deterministically from the generated storm severity and the data presented in Fig. 6. Supply node failures in both networks are generated as Bernoulli RVs independent of storm severity. If the required number of scenarios has not been reached, this process is repeated for the next scenario. Otherwise, the sets of link and node failure realizations are output for each scenario, along with the occurrence probability of that scenario. Algorithm 1 uses stratified sampling, a variance reduction technique. With Algorithm 1, we first divide the population of possible failure realizations into strata by hurricane severity, then sample asset failures for each category of hurricane. Similar works have employed other variance reduction techniques such as Latin Hypercube sampling [36,64] to ensure that the sampling covers a representative set of scenarios.

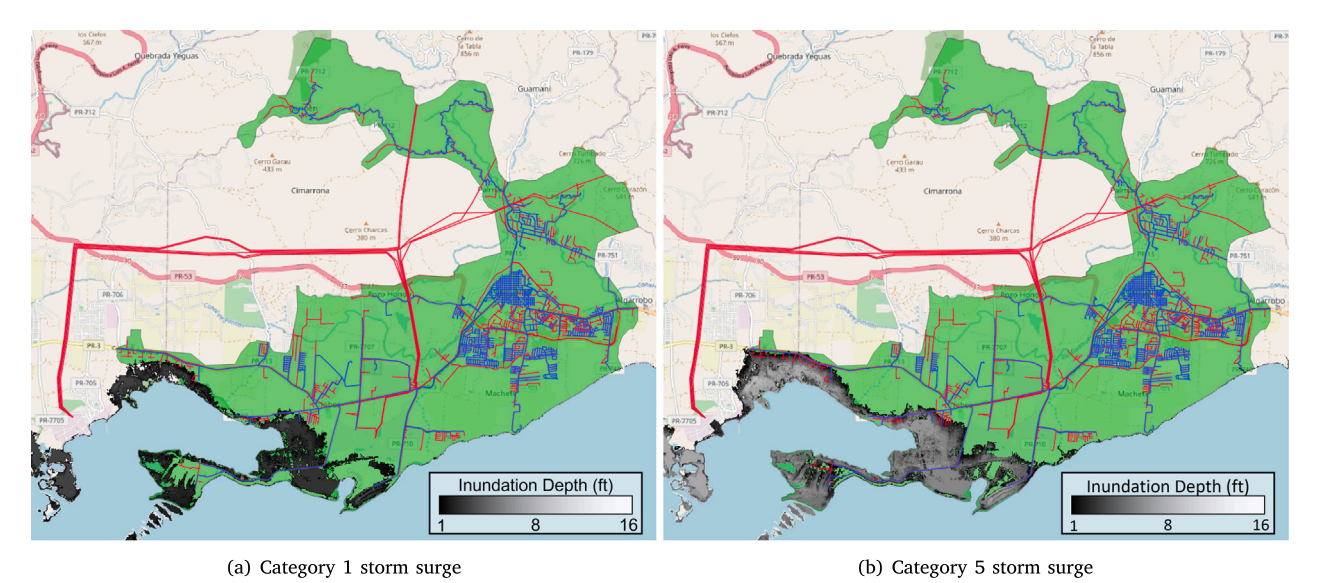


Fig. 6. Storm surge zone (gray) in the AOI. The power infrastructure is shown in red, the water infrastructure in blue, and the AOI in green.

Algorithm 1 Scenario Generation

- 1: **Input:** number of scenarios $|\Omega|$
- 2: **For** scenario ω in $|\Omega|$:
- 3: Generate hurricane category (discrete RV) with occurrence probability from historical hurricane data
- 4: Define W_s as the median wind gust speed for the simulated hurricane category
- 5: Calculate power link failure probabilities using (22)–(24)
- 6: Generate power line $(\xi_{ij\omega}^P)$ and power supply node $(\psi_{i\omega}^P)$ outages (Bernoulli RV)
- 7: Generate water pipe outages based on hurricane category and storm surge $(\xi_{ij\omega}^P)$
- 8: Generate water supply node outage $(\psi^P_{i\omega})$ realizations (Bernoulli RV)
- 9: **Return:** Post-disaster working capacity realizations $\psi_{i\omega}^s$, $\xi_{ii\omega}^s$

5. Results

We demonstrate our optimal hardening decision-making framework by implementing it on the Guayama power and water networks. The model defined by (1)-(19) was used to determine the optimal hardening decisions across 50 disaster scenarios. We implemented the model in Pyomo [65,66] and solved it using the Gurobi solver [67]. The original formulation selects hardening decisions based on direct consequences of the first stage decisions. The original formulation takes approximately 15 min to solve with the base case parametrisation on a Windows 10 laptop with 16 GB of RAM and an Intel(R) Core(TM) i7-8550U CPU @ 1.80 GHz processor. We then assessed the quality of the optimal hardening decisions using 1000 out-of-sample scenarios with the first stage hardening decisions (y_i^s) and z_{ij}^s fixed. For the out-of-sample experiments, we determined the decisions' performance on constraints defined by Eqs. (4)-(19) and the objective function defined by Eq. (25). With the first stage decisions fixed, the problem decomposes into separate optimization problems for the second stage decisions in each scenario. Thus, for each scenario, we computed the aggregate service loss using Eq. (25):

$$\min \sum_{\omega \in \Omega} p_{\omega} \left[\beta \sum_{i \in \mathcal{N}^W} \frac{u_{i\omega}^W}{\sum_{j \in \mathcal{N}^W} d_j^W} + (1 - \beta) \sum_{i \in \mathcal{N}^P} \frac{u_{i\omega}^P}{\sum_{j \in \mathcal{N}^P} d_j^P} \right]$$
 (25)

The original service level requirement, U, may not be met in all out-of-sample hurricane scenarios when the first stage decisions $(y_i^s \text{ and } z_{ij}^s)$

are fixed, requiring the reformulation for the out-of-sample assessment. We use β to represent the prioritization applied to the water network, and $(1-\beta)$ to capture the weight applied to the power network.

5.1. Base case

Parametrisation consistently presents challenges when building optimization models. For our most uncertain parameters, specifically the service level threshold, U, the repair cost factor, R, and the weighting between power and water demands, β , we perform sensitivity analyses exploring different values and their impacts on the optimal solution. For the base case, we first select a base value for each of these parameters, and explore the results for this case in more depth. For the base case, we assumed a service level requirement of U = 20%, a water weighting of $\beta = 50\%$, and a repair cost factor of R = 1.2. In reality, decision makers would set their own values for U and β , and R would be determined from actual costs. Our base values were selected to be approximately average across the parameter's range of possible values. With these base case assumptions, the optimal hardening decisions are shown in Fig. 7. Lighter links (blue for water, red for power) are unhardened, while darker links are chosen for some level of hardening. At optimality, all supply nodes are selected for hardening. These decisions cost \$1.81 million for hardening and an expected \$0.826 million for repairs. \$1.83 million is spent on the water network for both hardening and repairs, while \$0.807 million is spent on the power network. One supply node in each network is selected for hardening, as are 11 water pipes and 738 power lines. Because partial hardening is permitted, some assets are not hardened to their maximum capacity. We find that out of the 851 assets that are recommended for hardening, only 12 are hardened more than 90%. By contrast, 822 assets are recommended for a small amount (less than 20% hardening) of hardening. Very few assets receive a middling amount (between 20% and 90%) of hardening. In practice, this provides two useful pieces of information to decision makers. First, there are a few assets that decision makers should be certain to harden, and to harden them completely. For decision makers with little time to spend on a diffuse amount of hardening throughout the networks, this indicates which assets they should focus on. Second, there are many assets for which a small amount of hardening is optimal. For these assets, decision makers could consider more modest hardening activities, like inspections and tree-trimming for above-ground infrastructure. Overall, our assumption of linear hardening decisions yields results that suggest the degree of hardening decision makers should consider for all assets throughout the

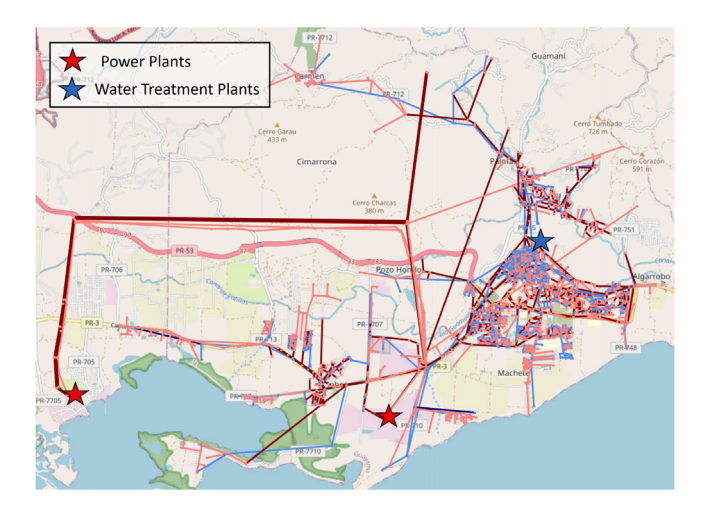


Fig. 7. Optimal power hardening decisions (dark red) and water hardening decisions (dark blue).

network. These results can help decision makers prioritize which assets to focus on for their hardening efforts.

For the base case, we find an Expected Value of Perfect Information (EVPI) of 14.6%, meaning even if the utility knew exactly which assets were going to fail in the next hurricane (i.e., had perfect information) and could harden accordingly, they would expect to save only 14.6% on hardening and repairs over the optimal hedging solution generated by the stochastic program. The EVPI is an upper bound on how much the utility would pay for information about the next disaster and its impacts. For example, utilities could more accurately estimate asset failure probabilities by inspecting assets for degradation or by studying historical asset failures. Practically however, because any information that the utility would gather would only marginally reduce uncertainty and because these activities would be relatively expensive (asset inspection in particular is challenging for underground infrastructure), investing in improved ability to predict disaster damages has limited value from a cost perspective.

The hardening decisions illustrated in Fig. 7 include a path from one of the power plants to the water treatment plant where all power lines are hardened. This helps ensure that power can be supplied to the water treatment plant, which is necessary for water supply and a prerequisite for operation of the water network. It also shows hardening of some of the longer links in the transmission infrastructure. Because longer links have a higher probability of failure, the preferential hardening of longer links follows intuition. Finally, Fig. 7 shows more hardening in the power network than the water network, both because it is more vulnerable to hurricanes, and because power link hardening is less expensive because the assets (power lines) are above-ground.

Fixing the hardening decisions in Fig. 7, we then simulated this hardening plan's performance on 1000 new hurricane scenarios, again using Algorithm 1. We determine the performance of the hardening decisions using the optimization problem defined by constraints (4)–(19)and the objective function (25) for each of the 1000 newly generated hurricane scenarios. The average aggregate service loss across these 1000 out-of-sample hurricanes is 1.03%, with a 95% confidence interval of [0.96%, 1.10%] and a maximum value of 5.93%. The narrow 95% confidence interval indicates that the 1000 out-of-sample scenarios are sufficiently many, so we continue to use 1000 out-of-sample scenarios throughout the remaining analyses. This maximum aggregate service loss is much lower than the threshold required by the original hardening problem, U = 20%, suggesting that the service level requirements that infrastructure system managers aim to achieve can reliably be satisfied despite uncertainty in potential hurricane realizations for the selected parametrisation. Fig. 8 shows the service level achieved for

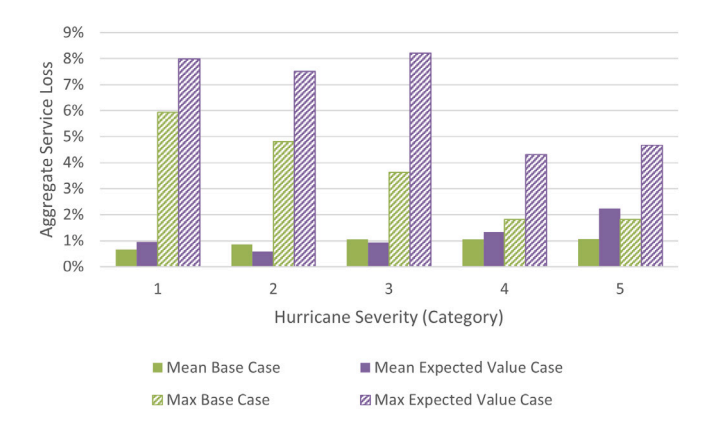


Fig. 8. Performance of the base case and expected value optimal hardening decisions on 1000 out-of-sample hurricane scenarios, for each category of hurricane.

different category hurricanes, both for the base case parametrisation and the expected value case. The expected value case sets each asset's failure realization ($\psi^s_{i\omega}$ and $\xi^s_{ij\omega}$) deterministically at their respective probabilities of failure and determines the optimal hardening decisions using Eqs. (1)-(19). The expected value case is a standard point of comparison in stochastic optimization. Fig. 8 shows that more demand is met for less severe hurricanes in the mean base case and mean expected value case, as would be expected. This trend does not hold for the maximum value of the base case and expected value case, likely because the maximum value is significantly more sensitive to the specific 1000 out-of-sample scenarios generated. In Fig. 8, the mean base case hardening performs similarly to the mean expected value case for less severe hurricanes, and outperforms the mean expected value case for the more severe hurricanes. The maximum base case also outperforms the maximum expected value case for all hurricane severities. This difference in performance helps validate the utility of our framework in the highly-uncertain disaster planning context; the expected value case does not sufficiently capture the range of potential disaster realizations, leaving the system more vulnerable to more extreme weather events and the potential for worse performance. We also compared the performance of our framework's hardening decisions against the case where no hardening is permitted. We found that without mitigation, repair costs were expected to be \$1.17 million. This value is less than the total cost (\$2.636 million) of hardening and expected recovery with optimal hardening decisions. However, no mitigation results in significantly higher expected unmet demand, with values as high as 35.5% and an expected unmet demand of 7.40%. Thus, without mitigation the expected unmet demand is higher than the maximum value experienced with mitigation (5.93%). The tradeoff between mitigation and recovery is explored in further detail in Section 5.3.

5.2. Service threshold

The selection of the service level requirement U is a challenge for any systems planner. If they select a service level that is too low, then they are exposing their customers to the brunt of the disaster impacts, forcing them to subsist without fundamental services while repairs are made in the wake of a disaster. If they select a service level that is too high, then more money will be spent on hardening projects than is necessary. In this sensitivity analysis, we explore the impact of the service level requirement U on the optimal hardening decisions while keeping the water prioritization as $\beta = 50\%$ and the repair cost factor as R = 1.2, as in the base case's parametrisation.

Fig. 9 shows the simulation results for the sensitivity analysis on service level requirement U. The results show that as the original service level requirement is relaxed, the aggregate service loss tends to

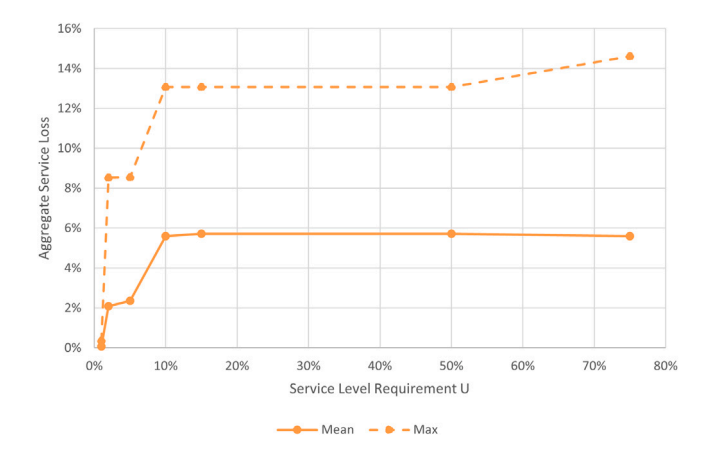


Fig. 9. Sensitivity analysis for the service level requirement U.

increase for both the maximum and mean values. This result indicates that the service level requirement U performs as it should, helping induce higher levels of reliability when dictated by the decision maker. Fig. 9 also shows that for less stringent service level requirements ($U \ge$ 15%) the maximum simulated service loss is lower than the original service level requirement U. However, for $U \ge 15\%$, the maximum aggregate service loss can exceed the service level requirement U, though the mean value did meet the requirement for all tested parameterizations. This indicates that the performance of hardening decisions is relatively robust to the service level requirement set by the decision maker for less stringent service level requirements. While the maximum service loss may exceed the original service level requirement U, the mean service loss is always bounded by the original service level requirement. Finally, plateauing behavior is exhibited for the mean aggregate service loss for $U \ge 15\%$. Our original formulation requires that the service level requirement U be met in every scenario, making investment highly sensitive to the worst-case scenario. The plateauing behavior indicates that the service level constraints (2) may no longer be as binding; this reasoning is confirmed by the fact that the out-ofsample maximum aggregate service loss is less than the service level requirement U for all parameterizations.

5.3. Repair costs

Because synthetic values were used to partially parameterize the hardening and repair costs in our model, we perform a sensitivity analysis to determine the potential impacts of our assumptions. We vary the repair cost parameter, R, which is defined in (20) and (21) as the multiplicative coefficient converting hardening costs to repair costs. A low R value indicates that hardening costs are higher than repair costs, and a high R value indicates repair costs are higher than hardening costs. Hardening and repair costs are equal when R = 1. In this experiment, we explore a single value of *R* for conversion between hardening and repair costs for all assets. In the literature, costs are highly dependent on location, type of hardening, degree of damage, and other factors [60]. Some hardening activities such as power line inspections and vegetation management are inexpensive compared to repair costs, while others like water line upgrades and power line undergrounding may be more expensive. Therefore, we test different values of R ranging over four orders of magnitude.

The impacts of repair cost factor R are explored in Fig. 10. On the right axis, repair costs increase dramatically as the repair cost factor, R, increases. Intuitively, it makes sense that as repair costs increase, more money is expected to be spent on repairs. Hardening costs also increase with R, as higher repair costs encourage more hardening investment to avoid high repair costs. Notably, aggregate service loss does not show a clear trend as R is perturbed; both high and low

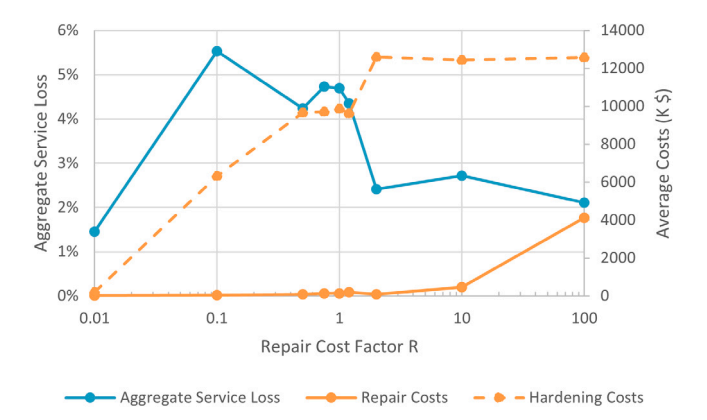


Fig. 10. Sensitivity analysis for the repair cost factor R.

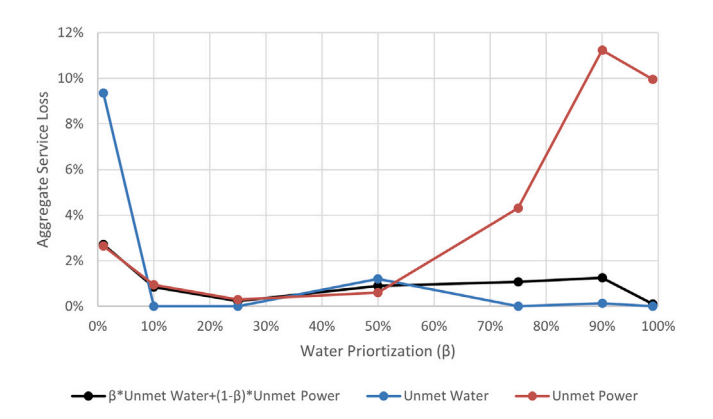


Fig. 11. Sensitivity analysis for the water prioritization parameter β . $\beta = 0\%$ indicates 100% power prioritization and $\beta = 100\%$ indicates 100% water prioritization.

values of *R* produce similar aggregate service loss. This suggests that the additional hardening, in this case driven by higher repair costs, does not necessarily translate to better service.

5.4. Power-water prioritization

Our formulation combines water and power decision-making into a single optimization framework. However, when assessing hardening performance through aggregate service loss (defined in Eq. (25)), decision makers have to determine the weighting of unmet water demand relative to unmet power demand. While both power and water unmet demands are normalized by total demand in their respective networks, it is possible that the value of lost service is higher for one infrastructure type than the other. For example, customers may have been able to store water in preparation for a disaster, so power outages could present a more immediate concern. We therefore explore the impacts of the prioritization of water service, β , on optimal hardening decisions and the resulting simulated achievable service levels and costs. For this experiment, we hold constant the base case parameter assumptions for the service level requirement (U = 20%) and the repair cost factor (R = 1.2).

Fig. 11 shows the trade-off between power and water service losses depending on the value of the water prioritization parameter β . $\beta=0\%$ indicates 100% power prioritization and 0% water prioritization while $\beta=100\%$ indicates 100% water prioritization and 0% power prioritization. For low values of β , service loss for water is much higher. Conversely, for high values of β , corresponding to high water service priority, service loss for power is high, while service loss for water is low. Fig. 11 reveals a region (10% $\leq \beta \leq 50\%$) over which the solution is fairly insensitive to the power-water prioritization. For all values of β ,

the aggregate service loss (black in Fig. 11) remains relatively constant. Service loss for power and water are not symmetric about $\beta=50\%$, producing lower service loss in the water network even for $\beta \leq 50\%$. This indicates that the power side may be more difficult to harden, both because the power network is longer (370 km as compared to the water network's 200 km) and because it is more vulnerable to hurricanes.

6. Conclusions

In this study, we explore the energy-water nexus in a disaster context. Natural disasters often exacerbate interdependencies between infrastructure systems, resulting in cascading failures. Natural disasters are becoming more frequent and severe, a trend driven by climate change. Infrastructure system managers aim to mitigate these effects by hardening CI to better withstand disasters, helping preserve service levels. The criticality of power and water to human life makes this not only a financial decision, but also an existential imperative. However, the uncertainty inherent in natural disasters poses a challenge to disaster planning. In this paper, we therefore develop a decision-making framework for infrastructure system managers designed to determine optimal hardening decisions across interdependent power and water networks. The optimization framework is a two-stage stochastic program, with infrastructure hardening as the first stage decisions, and network operation as the second stage decisions. Thus, guided by our model, the infrastructure system manager can hedge their hardening decisions with respect to a suite of potential natural disaster scenarios.

We implement the optimal decision-making framework for a case study focusing on the city of Guayama in Puerto Rico. Puerto Rico is highly vulnerable to hurricanes; the two Category 5 hurricanes, Irma and Maria, that struck the island in 2017 devastated infrastructure for months, leaving thousands without power and water. In our case study, we demonstrate that our optimal decision-making framework can be used effectively to make real-world hardening decisions. We find the following:

- 1. The decisions prescribed by our model favor hardening the power network; in the base case, all power lines connecting one of the power plants to the water treatment facility are hardened, helping to ensure that power is delivered to the origin of the water supply. The emphasis on hardening the power network over the water network is driven in large part by the power network's greater vulnerability to hurricanes; the entirety of the water network is buried, offering it some natural protection. The smaller scale of the water network combined with the one-way dependency of water on power also help explain this phenomenon.
- 2. We find an EVPI of 14.6% in the base case parametrisation. Practically, utilities would only be able to marginally reduce their uncertainty about exactly which assets are likely to fail in a disaster through activities like line and pipe inspections. Therefore, the EVPI of 14.6%, an upper bound on cost savings possible from these activities, suggests that data collection to reduce asset survival uncertainty would not hold much value to the decision maker from a system resilience perspective.
- 3. In the base parametrisation, we find that hedging with respect to the full set of possible disaster scenarios produces less variable aggregate service loss than planning only for the average hurricane scenario. We also find that this same hedging produces hardening decisions that perform better in the case of more severe hurricanes than planning only for the average hurricane scenario. Overall, these results show the necessity of the advanced treatment of uncertainty present in our formulation.
- 4. A tighter service level requirement in the planning stage improves the system's ability to provide service after a disaster. Additionally, hardening decisions are generally able to meet the service level requirement in out-of-sample assessments.

- 5. Significantly higher and significantly lower repair costs than hardening costs may lead to similar levels of aggregate service loss. Because higher repair costs encourage more hardening investment, this indicates that more hardening does not necessarily translate to reduced service loss.
- 6. The relative prioritization of water versus power service impacts the hardening decisions. While this conclusion is hardly unexpected, our model does reveal a fairly wide range over which the decisions are relatively insensitive to water versus power service prioritization. In general, our framework is able to demonstrate to decision makers the trade-offs between meeting service in the water network and meeting service in the power network, allowing them to select a prioritization that best suits their needs.

The findings enumerated above should be considered in tandem with the limitations of our formulation. Our model excludes some features that exist in reality; addressing these limitations suggests directions for future work. First, to ensure the tractability of the numerical study, the model defines hardening decisions as continuous. The most realistic representation would be an IP formulation with both integer and continuous decision variables describing specific hardening activities. Future work could relax our assumption of linearity, perhaps by identifying a subset of candidate links for hardening, thereby preserving tractability while also allowing discrete decision variables. A second limitation is the lack of energy balances in the power and water network modeling. We model both systems as generic commodities, ignoring pipe friction losses and reactive power. This could be of critical importance for a system under high stress during a disaster (e.g. balancing frequencies becomes challenging for a power grid system operating under disaster). Future research could address this limitation by modeling energy balances in addition to mass balances in the model. Finally, we aggregate time to a steady-state representation of post-disaster operations. Disaster resilience typically includes both a measurement of magnitude of service loss, which we do include, and an assessment of time spent without service, which our steady-state model lacks. Inclusion of multiple time periods in the model will significantly increase the computational intensity of the model, potentially requiring other simplifications to the model and making this extension a focus for future work.

CRediT authorship contribution statement

Rachel L. Moglen: Writing – review & editing, Writing – original draft, Visualization, Validation, Supervision, Project administration, Methodology, Investigation, Formal analysis, Data curation, Conceptualization. Julius Barth: Writing – review & editing, Methodology, Investigation, Formal analysis, Conceptualization. Shagun Gupta: Writing – review & editing, Methodology, Investigation, Formal analysis, Conceptualization. Eiji Kawai: Writing – review & editing, Investigation, Data curation, Conceptualization. Katherine Klise: Writing – review & editing, Supervision, Resources, Project administration, Funding acquisition, Data curation, Conceptualization. Benjamin D. Leibowicz: Writing – review & editing, Supervision, Resources, Project administration, Funding acquisition, Conceptualization.

Declaration of competing interest

The authors declare that they have no known competing financial interests or personal relationships that could have appeared to influence the work reported in this paper.

Data availability

Data will be made available on request.

Acknowledgments

Sandia National Laboratories is a multimission laboratory managed and operated by National Technology and Engineering Solutions of Sandia, LLC., a wholly owned subsidiary of Honeywell International, Inc., for the U.S. Department of Energy's National Nuclear Security Administration under contract DE-NA0003525. This paper describes objective technical results and analysis. Any subjective views or opinions that might be expressed in the paper do not necessarily represent the views of the U.S. Department of Energy or the United States Government. This work was supported by the Department of Energy's Office of Electricity and the Federal Emergency Management Agency (FEMA). This research was supported by the National Science Foundation of the U.S. through Award #1828974 (NRT-INFEWS: Graduate Student Education: Reducing Energy Barriers For Novel Water Supply Use in Sustainable Agriculture) granted to The University of Texas at Austin.

References

- [1] Ouyang Min. Review on modeling and simulation of interdependent critical infrastructure systems. Reliab Eng Syst Saf 2014;121:43–60.
- [2] Foundations Critical. Protecting America's infrastructures: The report of the President's commission on critical infrastructure protection. 1997, Washington, DC: The President's Commission on Critical Infrastructure Protection.
- [3] Aros-Vera Felipe, Gillian Shayne, Rehmar Austin, Rehmar Landon. Increasing the resilience of critical infrastructure networks through the strategic location of microgrids: A case study of Hurricane Maria in Puerto Rico. Int J Disaster Risk Reduct 2021;55:102055.
- [4] Busby Joshua W, Baker Kyri, Bazilian Morgan D, Gilbert Alex Q, Grubert Emily, Rai Varun, et al. Cascading risks: Understanding the 2021 winter blackout in Texas. Energy Res Soc Sci 2021;77:102106.
- [5] Campbell Richard J, Lowry Sean. Weather-related power outages and electric system resiliency. 2012, Congressional Research Service, Library of Congress Washington, DC.
- [6] Rus Katarina, Kilar Vojko, Koren David. Resilience assessment of complex urban systems to natural disasters: A new literature review. Int J Disaster Risk Reduct 2018;31:311-30
- [7] Levi Patricia J, Kurland Simon Davidsson, Carbajales-Dale Michael, Weyant John P, Brandt Adam R, Benson Sally M. Macro-energy systems: Toward a new discipline. Joule 2019;3(10):2282-6.
- [8] Panteli Mathaios, Mancarella Pierluigi. Influence of extreme weather and climate change on the resilience of power systems: Impacts and possible mitigation strategies. Electr Power Syst Res 2015;127:259–70.
- [9] Ghorbani-Renani Nafiseh, González Andrés D, Barker Kash, Morshedlou Nazanin. Protection-interdiction-restoration: Tri-level optimization for enhancing interdependent network resilience. Reliab Eng Syst Saf 2020;199:106907.
- [10] Bynum Michael, Staid Andrea, Arguello Bryan, Castillo Anya, Knueven Bernard, Laird Carl D, et al. Proactive operations and investment planning via stochastic optimization to enhance power systems' extreme weather resilience. J Infrastruct Syst 2021;27(2):04021004.
- [11] Gomez Camilo, Baker Jack W. An optimization-based decision support framework for coupled pre-and post-earthquake infrastructure risk management. Struct Saf 2019:77:1–9.
- [12] Cavdur Fatih, Kose-Kucuk Merve, Sebatli Asli. Allocation of temporary disaster response facilities under demand uncertainty: An earthquake case study. Int J Disaster Risk Reduct 2016;19:159–66.
- [13] He Xian, Cha Eun Jeong. Risk-informed decision-making for predisaster risk mitigation planning of interdependent infrastructure systems: Case study of Jamaica. J Infrastruct Syst 2021;27(4):04021035.
- [14] Pudasaini Binaya, Shahandashti Mohsen. Seismic rehabilitation optimization of water pipe networks considering spatial variabilities of demand criticalities and seismic ground motion intensities. J Infrastruct Syst 2021;27(4):04021028.
- [15] Klise Katherine A, Bynum Michael, Moriarty Dylan, Murray Regan. A software framework for assessing the resilience of drinking water systems to disasters with an example earthquake case study. Environ Model Softw 2017;95:420–31.
- [16] Aydin Nazli Yonca, Duzgun H Sebnem, Heinimann Hans Rudolf, Wenzel Friedemann, Gnyawali Kaushal Raj. Framework for improving the resilience and recovery of transportation networks under geohazard risks. Int J Disaster Risk Reduct 2018;31:832–43.
- [17] Karakoc Deniz Berfin, Almoghathawi Yasser, Barker Kash, González Andrés D, Mohebbi Shima. Community resilience-driven restoration model for interdependent infrastructure networks. Int J Disaster Risk Reduct 2019;38:101228.
- [18] Almoghathawi Yasser, Barker Kash, Albert Laura A. Resilience-driven restoration model for interdependent infrastructure networks. Reliab Eng Syst Saf 2019;185:12–23.

- [19] Javanbakht Pirooz, Mohagheghi Salman. A risk-averse security-constrained optimal power flow for a power grid subject to hurricanes. Electr Power Syst Res 2014;116:408–18.
- [20] Reilly Allison C, Samuel Andrew, Guikema Seth D. "Gaming the system": Decision making by interdependent critical infrastructure. Decis Anal 2015;12(4):155–72.
- [21] Zamzam Ahmed S, Dall'Anese Emiliano, Zhao Changhong, Taylor Josh A, Sidiropoulos Nicholas D. Optimal water-power flow-problem: Formulation and distributed optimal solution. IEEE Trans Control Netw Syst 2018;6(1):37–47.
- [22] Pereira-Cardenal Silvio J, Mo Birger, Gjelsvik Anders, Riegels Niels D, Arnbjerg-Nielsen Karsten, Bauer-Gottwein Peter. Joint optimization of regional water-power systems. Adv Water Resour 2016;92:200–7.
- [23] Sharma Neetesh, Nocera Fabrizio, Gardoni Paolo. Classification and mathematical modeling of infrastructure interdependencies. Sustain Resil Infrastructure 2021;6(1–2):4–25
- [24] Luiijf Eric, Nieuwenhuijs Albert, Klaver Marieke, van Eeten Michel, Cruz Edite. Empirical findings on critical infrastructure dependencies in Europe. In: International workshop on critical information infrastructures security. Springer; 2008, p. 302–10.
- [25] Utne IB, Hokstad P, Vatn J. A method for risk modeling of interdependencies in critical infrastructures. Reliab Eng Syst Saf 2011;96(6):671–8. http://dx.doi.org/ 10.1016/j.ress.2010.12.006, ESREL 2009 Special Issue.
- [26] Chang Stephanie E, McDaniels Timothy L, Mikawoz Joey, Peterson Krista. Infrastructure failure interdependencies in extreme events: Power outage consequences in the 1998 Ice Storm. Nat Hazards 2007;41(2):337–58.
- [27] McDaniels Timothy, Chang Stephanie, Peterson Krista, Mikawoz Joey, Reed Dorothy. Empirical framework for characterizing infrastructure failure interdependencies. J Infrastruct Syst 2007;13(3):175–84.
- [28] Barton Dianne C, Eidson Eric D, Schoenwald David A, Stamber Kevin L, Reinert Rhonda K. Aspen-EE: An agent-based model of infrastructure interdependency. 2000, SAND2000-2925. Albuquerque, NM: Sandia National Laboratories.
- [29] North Michael J. Multi-agent social and organizational modeling of electric power and natural gas markets. Comput Math Organ Theory 2001;7(4):331–7.
- [30] Dudenhoeffer Donald D, Permann May R, Manic Milos. CIMS: A framework for infrastructure interdependency modeling and analysis. In: Proceedings of the 2006 winter simulation conference. 2006, p. 478–85. http://dx.doi.org/10.1109/ WSC.2006.323119.
- [31] Leontief Wassily W. Input-output economics. Sci Am 1951;185(4):15–21, Full publication date: October 1951.
- [32] Gomez Camilo, González Andrés D, Baroud Hiba, Bedoya-Motta Claudia D. Integrating operational and organizational aspects in interdependent infrastructure network recovery. Risk Anal 2019;39(9):1913–29.
- [33] Duenas-Osorio Leonardo, Craig James I, Goodno Barry J. Seismic response of critical interdependent networks. Earthq Eng Struct Dynam 2007;36(2):285–306.
- [34] Lee II Earl E, Mitchell John E, Wallace William A. Restoration of services in interdependent infrastructure systems: A network flows approach. IEEE Trans Syst Man Cybern C (Appl Rev) 2007;37(6):1303–17.
- [35] Zuloaga Scott, Khatavkar Puneet, Vittal Vijay, Mays Larry W. Interdependent electric and water infrastructure modelling, optimisation and control. IET Energy Systems Integration 2020;2(1):9–21.
- [36] Alkhaleel Basem A, Liao Haitao, Sullivan Kelly M. Risk and resilience-based optimal post-disruption restoration for critical infrastructures under uncertainty. European J Oper Res 2022;296(1):174–202.
- [37] Shapiro Alexander, Dentcheva Darinka, Ruszczynski Andrzej. Lectures on stochastic programming: modeling and theory. SIAM; 2021.
- [38] Ouyang Min, Duenas-Osorio Leonardo. Multi-dimensional hurricane resilience assessment of electric power systems. Struct Saf 2014;48:15–24.
- [39] Kapusuzoglu Berkcan, Mahadevan Sankaran. Information fusion and machine learning for sensitivity analysis using physics knowledge and experimental data. Reliab Eng Syst Saf 2021;214:107712.
- [40] Tabandeh Armin, Sharma Neetesh, Gardoni Paolo. Uncertainty propagation in risk and resilience analysis of hierarchical systems. Reliab Eng Syst Saf 2022;219:108208.
- [41] Peeta Srinivas, Salman F Sibel, Gunnec Dilek, Viswanath Kannan. Pre-disaster investment decisions for strengthening a highway network. Comput Oper Res 2010;37(10):1708–19.
- [42] Liu Chuang, Ouyang Min, Wang Naiyu, Mao Zijun, Xu Xiaolin. A heuristic method to identify optimum seismic retrofit strategies for critical infrastructure systems. Comput-Aided Civ Infrastruct Eng 2021;36(8):996–1012.
- [43] Romero Natalia, Nozick Linda K, Dobson Ian, Xu Ningxiong, Jones Dean A. Seismic retrofit for electric power systems. Earthq Spectra 2015;31(2):1157–76.
- [44] Sarazin Gabriel, Morio Jérôme, Lagnoux Agnès, Balesdent Mathieu, Brevault Loïc. Reliability-oriented sensitivity analysis in presence of data-driven epistemic uncertainty. Reliab Eng Syst Saf 2021;215:107733.
- [45] Sharma Neetesh, Tabandeh Armin, Gardoni Paolo. Regional resilience analysis: A multiscale approach to optimize the resilience of interdependent infrastructure. Comput-Aided Civ Infrastruct Eng 2020;35(12):1315–30.
- [46] Kammouh Omar, Gardoni Paolo, Cimellaro Gian Paolo. Probabilistic framework to evaluate the resilience of engineering systems using Bayesian and dynamic Bayesian networks. Reliab Eng Syst Saf 2020;198:106813.

- [47] González Andrés D, Dueñas-Osorio Leonardo, Sánchez-Silva Mauricio, Medaglia Andrés L. The interdependent network design problem for optimal infrastructure system restoration. Comput-Aided Civ Infrastruct Eng 2016;31(5):334–50.
- [48] Cavdaroglu Burak, Hammel Erik, Mitchell John E, Sharkey Thomas C, Wallace William A. Integrating restoration and scheduling decisions for disrupted interdependent infrastructure systems. Ann Oper Res 2013;203(1):279–94.
- [49] El-Rayes Khaled, Moselhi Osama. Optimizing resource utilization for repetitive construction projects. J Constr Eng Manag 2001;127(1):18–27.
- [50] Zhang Yanlu, Yang Naiding, Lall Upmanu. Modeling and simulation of the vulnerability of interdependent power-water infrastructure networks to cascading failures. J Syst Sci Syst Eng 2016;25(1):102–18.
- [51] Government of Puerto Rico. Infrastructures geodata download. 2020, https: //gis.pr.gov/descargaGeodatos/Infraestructuras/Pages/default.aspx. [Accessed 30 September 2021].
- [52] Nan Cen, Sansavini Giovanni. A quantitative method for assessing resilience of interdependent infrastructures. Reliab Eng Syst Saf 2017;157:35–53.
- [53] Sharma Neetesh, Gardoni Paolo. Mathematical modeling of interdependent infrastructure: An object-oriented approach for generalized network-system analysis. Reliab Eng Syst Saf 2022;217:108042.
- [54] US Census Bureau. 2010 Census. 2011, US Department of Commerce.
- [55] Molina-Rivera Wanda L, Gómez-Gómez Fernando. Estimated water use in Puerto Rico, 2010. Technical report, U.S. Geological Survey; 2014, http://dx.doi.org/ 10.3133/ofr20141117.
- [56] USEnergy Information Administration. Electric power annual 2020. Technical report, US Energy Information Administration; 2021.
- [57] Watson Eileen B, Etemadi Amir Hossein. Modeling electrical grid resilience under hurricane wind conditions with increased solar and wind power generation. IEEE Trans Power Syst 2019;35(2):929–37.

- [58] Public Service Commission of Wisconsin. Underground electric transmission lines. Technical report, Public Service Commission of Wisconsin; 2011.
- [59] Eidinger John. Replacing seismically weak and aging water pipes. In: Proceeding of the 2nd Japan and US workshop on seismic measures for water supply. 2001.
- [60] Brown RE. Cost-benefit analysis of the deployment of utility infrastructure upgrades and storm hardening programs. 2009, Quanta Technology, Raleigh.
- [61] National Oceanic and Atmospheric Administration. Historical hurricane tracks. 2021.
- [62] Arrighi Chiara, Tarani Fabio, Vicario Enrico, Castelli Fabio. Flood impacts on a water distribution network. Nat Hazards Earth Syst Sci 2017;17(12):2109–23.
- [63] Zachry Brian C, Booth William J, Rhome Jamie R, Sharon Tarah M. A national view of storm surge risk and inundation. Weather Clim Soc 2015;7(2):109–17.
- [64] Alkhaleel Basem A, Liao Haitao, Sullivan Kelly M. Model and solution method for mean-risk cost-based post-disruption restoration of interdependent critical infrastructure networks. Comput Oper Res 2022;144:105812.
- [65] Hart William E, Laird Carl D, Watson Jean-Paul, Woodruff David L, Hackebeil Gabriel A, Nicholson Bethany L, et al. Pyomo-optimization modeling in Python, vol. 67. Springer; 2017.
- [66] Hart William E, Watson Jean-Paul, Woodruff David L. Pyomo: Modeling and solving mathematical programs in Python. Math Program Comput 2011;3(3):219–60.
- [67] Gurobi Optimization LLC. Gurobi optimizer reference manual. 2022.